Micro-CT and Finite Element Analysis of Dentin Preservation and Stress Distribution in Mesial Roots of Mandibular Molars after Shaping with Different Tapers

Micro-CT and Finite Element Analysis of Dentin Preservation and Stress Distribution in Mesial Roots of Mandibular Molars after Shaping with Different Tapers

Mario Alovisi, DDS, PhD,[*]
Andrea Baldi, DDS, PhD,[*]
Edoardo Moccia, DDS, PhD,[*]
Ivan Gaviglio, PhD,[†]
Allegra Comba, DDS, PhD,[*]
Lia Giordano, DDS,[*]
Nicola Scotti, DDS, PhD,[*] *and*
Damiano Pasqualini, DDS[*]

ABSTRACT

Introduction: The aim of this study was to evaluate the dentin preservation and fracture resistance of mandibular molar mesial roots after shaping with different tapers using micro–computed tomography (micro-CT) and finite element analysis (FEA). **Methods:** Forty-eight mandibular first molars with independent mesial canals were selected. The mesio-lingual and mesio-buccal canals were randomly assigned ($n = 12$) to ProTaper Gold (PG), ProTaper Next (PTN), ProTaper Ultimate (PTU), and B4U instrumentation systems. Pre- and post-shaping micro-CT scans were performed to compare root canal volume and cervical dentin volume. The centroid shift and the percentage and distribution of the dentin removal in correspondence of the mesial canals were analyzed in coronal, middle, and apical points of analysis and below the furcation at the "danger zone." The residual dentin thickness in the distal and mesial aspects of the mesial canals was measured. A linear elastic model of a mesial root of a mandibular molar was created through the finite element method (FEM) and a 200N perpendicular load was applied on the root canal coronal third. One-way factorial analysis of variance with Bonferroni correction and post hoc Tukey-Kramer tests were used ($P < .05$). **Results:** The mean cervical dentin volume removal was statistically lower for the B4U compared with the PG system ($P < .05$). The canal centering ability was statistically more accentuated for the B4U group in the coronal and middle third and higher centroid shift variations occurred for PG system ($P < .05$). The residual dentin thickness appeared statistically higher after shaping with B4U through the mesial and distal root aspect at the coronal point of analysis and at the danger zone ($P < .05$). PG removed more dentin in the coronal root canal third ($P < .05$). The FEM analysis showed no statistically significant differences between groups ($P > .05$). **Conclusions:** The reduction of the root canal taper may improve the instruments' centering ability and the preservation of the residual dentin tissue, especially in the coronal and middle third. The root canal taper seems not to influence the stress distribution pattern through the mesial root of the lower molars. *(J Endod 2025;51:1477–1484.)*

KEY WORDS

Canal shaping; finite element analysis; mandibular molar; micro–computed tomography; rotary systems; stress distribution

SIGNIFICANCE

Minimally invasive endodontic principles lead to lower tapered preparations. This study addresses that the reduction of the canal taper may improve the instruments' centering ability not influencing the stress distribution pattern through the mesial root of the lower molars.

The maintenance of tooth dentinal structure appears crucial for the long-term endodontic prognosis[1-3]. It is widely assumed that the thickness of the residual radicular dentin is crucial for the long-term survival of endodontically treated teeth[4,5]. In particular, the preservation of the dentinal cervical collar seems mandatory for tooth resistance[6].

Endodontic shaping instruments are becoming less invasive with a reduced taper and increased flexibility[7,8]. The new nickel-titanium (NiTi) alloys and instrument geometries allow minimally invasive preparations with a systematic respect for the original dental tissue[9]. The reduction of the

From the *Department of Surgical Science, Dental School, University of Turin, Turin, Italy; and †Engineering Private Practice, Turin, Italy

Address requests for reprints to Prof Mario Alovisi, Department of Surgical Science, Dental School, University of Turin, via Nizza, 230–10126, Torino, Italy.
E-mail address: mario.alovisi@unito.it
0099-2399

https://doi.org/10.1016/j.joen.2025.06.017

taper during shaping should have some advantages in terms of tissue preservation, without reducing the quality of root canal disinfection and filling[10,11]. In particular, a low-tapered preparation is indicated in the mesial canals of the mandibular molars, due to the presence of a danger zone below the furcation where the dentin thickness is minimal[12-14]. Furthermore, the mandibular molars are prone to fracture after extensive coronal tissue loss and excessive removal of dentin in the coronal portion during shaping[15]. However, the effect of root canal taper on the fracture resistance of the mandibular molars is still controversial[16].

Recently, several rotary endodontic shaping systems have been proposed, with different geometries, sections, and alloys. Even though they are systems with a progressive taper, the ProTaper Gold system (Dentsply Maillefer, Ballaigues, Switzerland) displays a 0.09 mean preparation taper, whereas the ProTaper Ultimate (Dentsply Maillefer) and ProTaper Next (Dentsply Maillefer) create a shaping of respectively 0.08 and 0.06 taper. Recently, the B4U system (Sweden & Martina, Padua, Italy) was proposed to fulfill the concept of a reduced tapered preparation reaching a 0.05 final taper.

The aim of this study was to compare different shaping systems with distinct mean preparation tapers in terms of canal centering ability, preservation of the root canal dentinal tissue, and root fracture resistance through micro–computed tomography (micro-CT) and finite element analysis (FEA). The null hypothesis is that different shaping tapers do not influence the canal anatomy preservation and stress distribution on the mesial roots of mandibular first molars in FEA simulation.

MATERIALS AND METHODS

This article was written according to the Preferred Reporting Items for Laboratory studies in Endodontology (PRILE) 2021[17]. The study was approved by the local research ethics committee (approval code CS2_1053_2022).

Specimen Selection

A total of 140 permanent mandibular first molars, not previously subjected to endodontic treatment, free of caries, and freshly extracted for periodontal disease, were selected in accordance with the local ethics committee. A sample size of 12 per group was calculated with G*Power 3.1.4 (Kiel University, Kiel, Germany) to set the study power at 80% (a large effect size of 1 was considered for the sample size computation). After the root debridement with Gracey curettes, the specimens were immersed in a 0.01% sodium hypochlorite (NaOCl) solution at 4 °C for 24 h (Niclor 5, OGNA, Muggiò, Italy) and then stored in saline solution until experimental use.

Inclusion Criteria

Specimens were placed on a custom holder and micro-CT scanned (SkyScan 1172 micro-CT, Bruker, Kontich, Belgium) at low resolution (27.45 μm, 100 kV, 100 μA) to obtain overall information regarding the root canal anatomy. Images were reconstructed using NRecon software (Bruker, Kontich, Belgium), exporting the files in DICOM (.dcm) format.

The morphological parameters of the mesio-lingual (ML) and mesio-buccal (MB) canals were obtained, and the following inclusion criteria were applied. First mandibular molars with fully formed root apices and 2 independent mesial canals along their entire length were selected. The ML and MB canals measured 12 ± 2 mm from canal orifices to the apical foramen and showed 20 to 40° primary root canal curvature in bucco-lingual projection according to the Schneider method[18]. The main curvature radius was selected $4 < r \leq 8$ mm, with a point of maximum curvature located at the middle third. The proximal curvature was investigated from a mesio-distal projection and only teeth with a 10 to 30° primary curvature were considered[19]. Teeth with significant root canal calcifications were excluded, as well as teeth with a third median canal in the mesial root. Teeth not concurring with the inclusion criteria regarding canal curvature and patency were excluded.

Micro-CT Analysis

Forty-eight elements were selected in accordance with the inclusion criteria. The remaining specimens were discarded due to anatomical features or severe root canal calcifications. A traditional endodontic access (TEC) was performed with an 880-314-012 diamond cylindrical bur (Komet, Gebr. Brasseler GmbH & Co KG, Lemgo, Germany) to remove all the coronal interferences[20].

Afterward, each sample was scanned at high resolution with the following micro-CT parameters: 100 kV and 100 μA, isotropic resolution equal to 20.86 μm/pixel, in a time frame of about 2 h for each sample. The scan was performed with a rotation step of 0.7° and a frame averaging of 4, with sample rotation of 360°, using an aluminum and copper filter. Each scan produced, on average, 1031 cross sections per sample, saved in .tiff format at a resolution of 1000 × 666 pixels. The images were reconstructed using the NRecon software and the root canal anatomies were analyzed with high-resolution 3-dimensional (3D) rendering and orthogonal cross sections to assess homogeneity of the groups at baseline (cross-sectional areas and diameters 1 mm from apical foramen and root canal volume). After checking the normality assumption (Shapiro-Wilk test), the degree of homogeneity was evaluated by 1-way analysis of variance (ANOVA) (level of significance 5%).

Then, through Materialise Mimics 24.0 software (Materialise NV, Leuvren, Belgium) the following parameters were evaluated for each specimen: cervical dentin volume (CDV), centroid shift, and the dentin thicknesses proximal to the mesial canals, both in the mesial and distal directions.

Specimen Preparation

Ninety-six root canals were selected for the study. The manual canal scouting of both ML and MV canals with a K-File #10 (Dentsply Maillefer) was performed for all the specimens up to working length (WL), using Glyde (Dentsply Maillefer) as the lubricating agent (0.80 mg)[21]. The WL was determined under ×10 magnification (OPMI Pro Ergo, Carl Zeiss, Oberkochen, Germany) when the tip of the instrument was visible at the apical foramen. For all specimens, the mechanical glide path was completed with NiTi rotary ProGlider (Dentsply Maillefer) using an endodontic motor (X-Smart Plus, Dentsply Maillefer) with 16:1 contra angle at 300 rpm, 4 Ncm at full WL. Then the canals were randomly assigned to 4 different groups ($n = 24$) according to the shaping technique using a computer-generated randomization system. The glide path and shaping were performed with 4 different rotary systems following the direction for use: ProTaper Gold (PG) (Dentsply Maillefer) up to F2 (25/0.08), ProTaper Ultimate (PTU) (Dentsply Maillefer) up to F2 (25/0.08), ProTaper Next (PTN) (Dentsply Maillefer) up to ×2 (25/0.06), and B4U (Sweden & Martina) up to Finisher (23/0.05). The instruments were removed and cleaned each time after 3 pecking motions until WL was reached. The shaping was performed using an endodontic motor (X-Smart Plus, Dentsply Maillefer) with 16:1 contra angle following the specific direction for use. The irrigation was ensured

TABLE 1 - The Mean Number of Elements and Nodes of the Finite Element Models

	PG	PTN	B4U	PTU
Mean number of nodes	41,696	40,189	39,862	43,071
Mean number of elements	173,027	172,112	171,622	174,153

PG, ProTaper Gold Group; PTN, ProTaper Next Group; PTU, ProTaper Ultimate Group.

alternating 5% NaOCl (Niclor 5, OGNA, Muggiò, Italy) and 10% EDTA (Tubuliclean, OGNA) for a total of 5 mL for each solution for each canal using a 30G needle up to the apical third. Recapitulation with a size 10 K-File was performed between each instrument. Afterward, the root canals were dried with absorbent sterile paper points and micro-scanned for posttreatment-analyses. The procedures were led by a single expert operator with more than 10 years of practice in endodontics who was familiar with all the rotary systems used and who avoided intentional brushing movements.

Micro-CT Imaging Analysis

The 3D models before and after shaping were matched to enable pre- and postoperative evaluation for each group. The 3D and bi-dimensional (2D) analyses were performed automatically through the software CTAn (Bruker, Belgium) to reduce manual errors. The CDV was determined collecting the 3D dentinal amount circumferentially to the canal lumen from 2 mm coronal to 2 mm apical to the furcation for a total height of 4 mm below the cementum-enamel junction. Moreover, 2D analyses were evaluated on cross-sectional images. The centroid shift was analyzed in coronal (C), middle (M), and apical (A) points of analysis and the percentage and the distribution of dentin removal at the mesial canals were analyzed also below the furcation at the "danger zone" (D). The point of analysis C was set at the middle portion of the root canal coronal third defined by a 3D calculation of the root canal length from the orifice to the foramen; the M was set at the point of the maximum curvature and A 1 mm from the apical foramen. The different points of analysis were selected as representative of the critical shaping points[22]. The residual dentin thickness in the distal and mesial aspects of the mesial canals was measured. The same plane was used for pre- and postoperative cross-section orientation perpendicular to the canal axis. Axial slices were imported and automatically analyzed with the CTAn software to evaluate the minimal distance between the root canal lumen and the mesial and distal aspects of the root canal surface. An automated threshold was implemented for all the slices to avoid manual errors[23].

FEA Method

For the FEA, 1 single tooth element for each group was numerically discretized. In particular, the sample that showed the worst results in terms of cervical dentin removal, centroid shift, and remaining tooth structure at the points of analysis was selected. Specifically, the following parameters were evaluated: Δ centroid shift, Δ root canal volume, Δ cervical dentin removal, and Δ remaining tooth structure at the mesial and distal aspect of the analyzed root canals. This method was selected due to the possibility of analyzing the worst scenario through FEM. The pre- and post-shaping DICOM files for each selected sample were used[24]. The files were imported in the software Materialise Mimics 24.0 (Materialise NV, Leuven, Belgium) to create STL files. Thanks to the different radiodensities of the dental elements, multiple pixel segments were created of the different hard tissues in contrast with the canal lumen. Considering that the aim was to evaluate the distribution of the stresses at the cervical root level, the coronal tooth portion at the level of the furcation was removed. Post-processing morphological automatic operations were performed to ensure the correct superimposition between the different masks. Then, the obtained STL files were imported into 3-Matic Medical 20.0 (Materialise NV) to perform a mesh finishing process in which a decimation process of the finite elements was carried out and degenerated elements were deleted. In addition, the holes created in the solid were filled and the normal elements were reoriented in the same direction as the other elements, making the mesh suitable for the volume of the created elements. The 2D element model was subsequently converted into a tetrahedral mesh through the software Altair Hyperworks (Altair Engineering, Troy, MI, USA). The mean number of elements and nodes of the finite element models is reported in Table 1. For each analyzed sample, the different tooth tissues were analyzed with a linear elastic material model.

A static analysis was carried out, all the elements were considered to be isotropic, and for each tissue a specific Young elasticity modulus and Poisson coefficient were established[25,26]. This represents the degree of shrinking or dilating transversally in the presence of a longitudinal monodirectional stress.

A standard force of 200N (mean chewing force) was applied perpendicular to the roof surface at the level of the furcation floor and evenly distributed. The analysis was carried out recording the equivalent von Mises stress distribution and the maximum shear stress for each model, before and after shaping at the points of analysis C, M, and A. Moreover, the directions of the principal tensions through the root surface were analyzed pre- and post-shaping at the point of analysis D.

Statistical Analysis

Data distribution was analyzed with the Shapiro-Wilk normality test. Differences in centroid shift and residual dentinal thickness at the levels of analysis were analyzed through the Mann-Whitney test and Bonferroni correction ($P < .05$). One-way ANOVA and post hoc Tukey-Kramer test ($P < .05$) were used to analyze differences in root canal volume and cervical dentinal volume. The same analysis was used to evaluate the impact of the instrumentation on the FEM stress distribution ($P < .05$).

TABLE 2 - Sample Baseline Characteristics in all Groups (Mean, SD)

	PG	PTN	B4U	PTU	*P*
Canal volumes (mm^3)	2.11 ± 0.67	2.26 ± 0.87	1.99 ± 0.92	2.17 ± 1.09	.21
Canal surface area (mm^2)	15.52 ± 2.87	16.85 ± 3.05	15.09 ± 2.67	16.21 ± 2.17	.17
Apical diameters* (mm)	0.17 ± 0.08	0.19 ± 0.12	0.16 ± 0.11	0.18 ± 0.09	.29

PG, ProTaper Gold Group; PTN, ProTaper Next Group; PTU, ProTaper Ultimate Group.
Statistical significance indicated by $P < .05$.
*Apical diameters (Mean ± SD) at 1 mm from apical foramen.

RESULTS

The mean curvature of the mesial root canals was 33.43° in the different groups with no

TABLE 3 - Mean and Standard Deviation of Cervical Volume Differences Between Groups

Cervical dentin volume differences (μm^3)	Mean	SD	*P*
ProTaper Gold (PG)	8.515	3.841	.007
ProTaper Next (PTN)	6.374	1.548	.09
B4U	4.480	2.445	.006
ProTaper Ultimate (PTU)	6.025	1.953	.11

Statistical significance indicated by $P < .05$.

statistically significant differences ($P > 0.5$). There was no incidence of instrument fracture during canal preparation. Canal volumes, surface areas, and mean apical diameters at baseline are presented in Table 2. The values displayed preoperative homogeneity between groups ($P > .05$).

3D Analysis

CDV differences between pre- and post-shaping are presented in Table 3. The analysis of the root canal cervical volumes displayed a statistically higher dentinal removal for the PG group ($P = .007$), whereas the group B4U resulted in a lower amount of removed dentin compared with the other techniques ($P = .006$). No statistically significant differences were noticed between the PTU and PTN groups ($P > .05$).

2D Analysis

Results of the centroid shift in the ML and MB canals are showed in Table 4. The analysis of the centroid shift reported that in the point of analysis C, the B4U group showed a lower alteration of the original canal anatomy ($P = .047$). In the point of analysis M, the same result was achieved by B4U ($P = .023$), whereas the PG group displayed a significantly higher centroid shift compared with the other groups ($P = .021$). The other comparisons were not significant.

The analysis of the remaining dentin thicknesses at the distal root canal aspect reported that at the point C, B4U showed less removal of dentin ($P = .009$) and the PG showed higher ($P = .013$) compared with other groups. At the point of analysis D, B4U appeared statistically more conservative ($P = .017$). No differences were noticed at the point of analysis M and A (Table 5).

The analysis of the remaining dentin thickness at the mesial root canal aspect reported that at the point C, B4U seemed to remove the least amount of dentin ($P = .033$), whereas no differences were reported between the other shaping techniques ($P > .05$). The same trend was highlighted for the point of analysis D ($P = .021$). At the point M, PG removed a significantly higher amount of dentin ($P = .012$) and B4U a lower amount ($P = .038$). No differences were noticed at the point of analysis A (Table 4).

Comparing the overall results between ML and MV canals, the MV canals exited in a significantly higher dentin removal through the mesial root aspect in the points of analysis C ($P < .001$) and D ($P < .001$). No other differences were reported regarding 3D and 2D analyses.

FEM Analysis

The analysis of the pre- and postoperative equivalent von Mises stress distribution in the groups showed no statistical differences for any shaping technique ($P > .05$). In the PG group, a slight increase of the von Mises stresses has been noticed at the point of analysis C and M, where the dentin thickness toward the distal root aspects is reduced ($P > .05$) (Fig. 1). Similarly, the PTN group showed an increase in the stress distribution at the point of analysis M, even though not statistically significant ($P > .05$) (Fig. 1). In the groups PTU and B4U, no significant differences between pre- and post-shaping analyses were noticed ($P > .05$) (Fig. 1). The vectors distribution of the shear forces has been analyzed and no differences were displayed for each group ($P > .05$) (Fig. 2). In correspondence of the MB canal of the PG model ($P = .021$) and the ML canal of the PTN model ($P = .04$), the tensions distribution showed significant increase, indicating a slight weakening of the point of analysis D (Fig. 2).

TABLE 4 - Centroid Shift (Mean, SD) at Coronal (C), Middle (M), and Apical (A) Points of Analysis

	C		M		A	
Centroid shift (μm)	Mean	SD	Mean	SD	Mean	SD
ProTaper Gold (PG)	0.136^a	0.095	0.132^a	0.085	0.104^a	0.079
ProTaper Next (PTN)	0.168^a	0.111	0.081^b	0.055	0.103^a	0.082
B4U	0.110^b	0.104	0.069^c	0.047	0.094^a	0.062
ProTaper Ultimate (PTU)	0.152^a	0.111	0.129^b	0.106	0.076^a	0.045

Different superscript letters (^{a,b,c}) in the same column indicate significant differences between groups ($P < .05$).

DISCUSSION

This study evaluated the influence of the taper on the root canal centering ability and fracture strength. The micro-CT analysis reported an increased amount of removed dentin tissue after shaping with instruments with a higher taper; however, this aspect should not influence the fracture strength of the mesial root of the first mandibular molars.

A traditional endodontic access seems not to adversely affect residual tooth structures and the overall outcome of endodontic treatment[6]. Furthermore, excessive decrease in the extent of the access cavity does not always lead to mechanical and biological benefits, especially when one or more tooth walls have already been lost[20]. In particular, especially in mandibular molars, an excessive conservative endodontic access could lead to a deterioration in the quality of shaping procedures, leading to unnecessary bending of the instruments and uneven distribution of forces within the intra-canal dentinal framework[14].

Otherwise, the preservation of the CDV is fundamental for the long-term outcome of the endodontically treated teeth, and excessive tissue removal could predispose to a subsequent root fracture[27-29]. Therefore, recently the endodontic NiTi instruments are becoming even more minimally invasive[30]. Moreover, the reduction of operative time and the simplification of the shaping sequences with respect to the endodontic biological and mechanical objectives are demanded[30]. However, there is not agreement on the effect of the preparation taper on the fracture resistance of the mesial roots of the mandibular molars.

Frequently, the mesial roots of the mandibular molars are prone to fracture because of their peculiar anatomy[13,31]. The presence of a "danger zone" below the furcation of the mandibular molars must be considered during shaping[13]. Therefore, the maintenance of an adequate sound tissue

TABLE 5 - Remaining Dentin Thickness at the Distal Root Aspect (Mean, SD) at Danger Zone (D), Coronal (C), Middle (M), and Apical (A) Points of Analysis

	D		C		M		A	
	Distal	Mesial	Distal	Mesial	Distal	Mesial	Distal	Mesial
	Mean ± SD	Mean ± SD	Mean ± SD	Mean ± SD	Mean ± SD	Mean ± SD	Mean ± SD	Mean ± SD
ProTaper Gold (PG)	19.75 ± 9.88[a]	16.55 ± 11.32[a]	19.62 ± 14.08[a]	13.25 ± 9.75[a]	17.08 ± 9.94[a]	14.13 ± 6.16[a]	13.57 ± 9.52[a]	14.19 ± 8.03[a]
ProTaper Next (PTN)	16.95 ± 8.21[a]	18.13 ± 8.37[a]	14.95 ± 11.93[b]	9.86 ± 7.19[a]	15.56 ± 9.41[a]	12.26 ± 6.59[b]	17.02 ± 13.14[a]	16.27 ± 11.50[a]
B4U	11.23 ± 6.58[b]	8.59 ± 6.44[b]	8.11 ± 5.32[c]	7.92 ± 6.68[b]	17.02 ± 13.13[a]	6.77 ± 5.33[c]	14.369 ± 12.29[a]	13.64 ± 8.48[a]
ProTaper Ultimate (PTU)	15.113 ± 9.25[a]	11.65 ± 6.74[a]	13.15 ± 11.02[b]	11.10 ± 5.72[a]	15.44 ± 7.90[a]	9.95 ± 7.41[b]	12.724 ± 7.34[a]	15.59 ± 7.58[a]

Different superscript letters ([a,b,c]) in the same column indicate significant differences between groups ($P < .05$).

volume centered in the root canal is requested to overcome procedural errors[14].

The centering ability of the shaping instruments is widely analyzed through micro-CT scans[9]. The micro-CT analysis represents a reproducible and nondestructive method for the evaluation of shaped root canals with shaping instruments[32]. The alignment of the datasets obtained by the volumetric renderings allows the 3D analysis of the canal volume and the 2D analysis of the orthogonal root canal sections[33,34]. However, this analysis does not provide information about the fracture resistance of the treated elements.

The FEM analysis allows for better evaluation of internal stress distribution and ensures standardization between models compared with other methods. However, the variability and complexity of the canal anatomy cannot always be correctly represented through a mathematical model. Thus, it is possible to perform an accurate analysis using data from 3D scans of the instrumented dental elements after the development of proper digital image techniques[35].

Multiple studies assess the risk of fracture through FEM[36]. A structural failure can occur when von Mises tension exceeds the tooth resistance. In the FEM, the site of maximum stress is the point where cracks are most likely to be formed due to excessive load concentration[36]. The FEM analysis can simulate the effect of shaping parameters of the mesial canals in a scenario that tries to mimic the clinical situation. Also, it overcomes some of the *ex vivo* test limitations, such as the standardization of the specimens, avoiding possible variations in dentin mechanical properties, storage time, and tooth extraction forces. In the study of Sathorn et al[37], an FEA was carried out to evaluate the distribution of stress on a lower shaped incisor with different tapered instruments and it was found that the propagation of dentin cracks is perpendicular to the surface where maximum stress is located.

Although the coronal factor is indicated as an important variable to be considered for the stress propagation, the effect of a low-tapered preparation on the preservation of the periradicular dentin and on the tooth fracture resistance is still controversial. Since their introduction, NiTi instruments have undergone remarkable changes in the alloy characteristics, especially by the mechanical and thermal treatments during processing[38]. These features, combined with the different types of movement, led to an increased maintenance of the original anatomy and reduced invasiveness[38].

The ProTaper Gold technology includes the same geometries as ProTaper Universal with advanced metallurgies and increased flexibility. ProTaper Next presented an off-centered, rectangular cross-section with the rotation axis that differs from the center of mass[9]. ProTaper Ultimate maintained several similarities compared with the previous generations of ProTaper, with different NiTi alloys, variable taper, and parallelogram cross section to improve the instrument's flexibility. Otherwise, the design criteria of the B4U showed different NiTi alloys, lower taper, rhomboidal cross section, and variable helix angles.

According to a previous study published by Keles et al[39], in this study the results showed a remarkable preservation of the cervical after shaping with a reduced taper. Similarly, the root canals shaped with PG showed a higher cervical tissue removal and a greater dentinal preservation was found in the B4U group. Therefore, the B4U system seemed more conservative, preserving a greater amount of dentin on the mesial and distal root aspect at the level of the coronal middle point and at the danger zone.

The analysis of the displacement of the centroid line also showed statistically significant differences between groups. In particular, the PG group showed a greater shift at the point of analysis M. Otherwise, B4U showed a higher centering ability both in the coronal and middle root canal third. These results could be related to a low-tapered shape and to a greater flexibility of the rhomboidal cross-section of these NiTi files.

Analyzing the differences between ML and MB canals, the latter showed a greater decurtation of dentin tissue on the mesial side at the points of analysis M and D. The 3D anatomy of the coronal and middle third of the MB canals suggests a more accentuated difficulty during access and a higher risk of coronal interferences[13].

Although the samples shaped with high tapered instruments underwent a greater removal of the cervical dentin, there were no significant variations in fracture resistance. Therefore, a more aggressive shaping (taper 0.08) seemed not to be significant regarding the root strength. Although the coronal factor has been excluded from this study, it can be concluded that the different types of instrumentation do not reduce the resistance of the tooth.

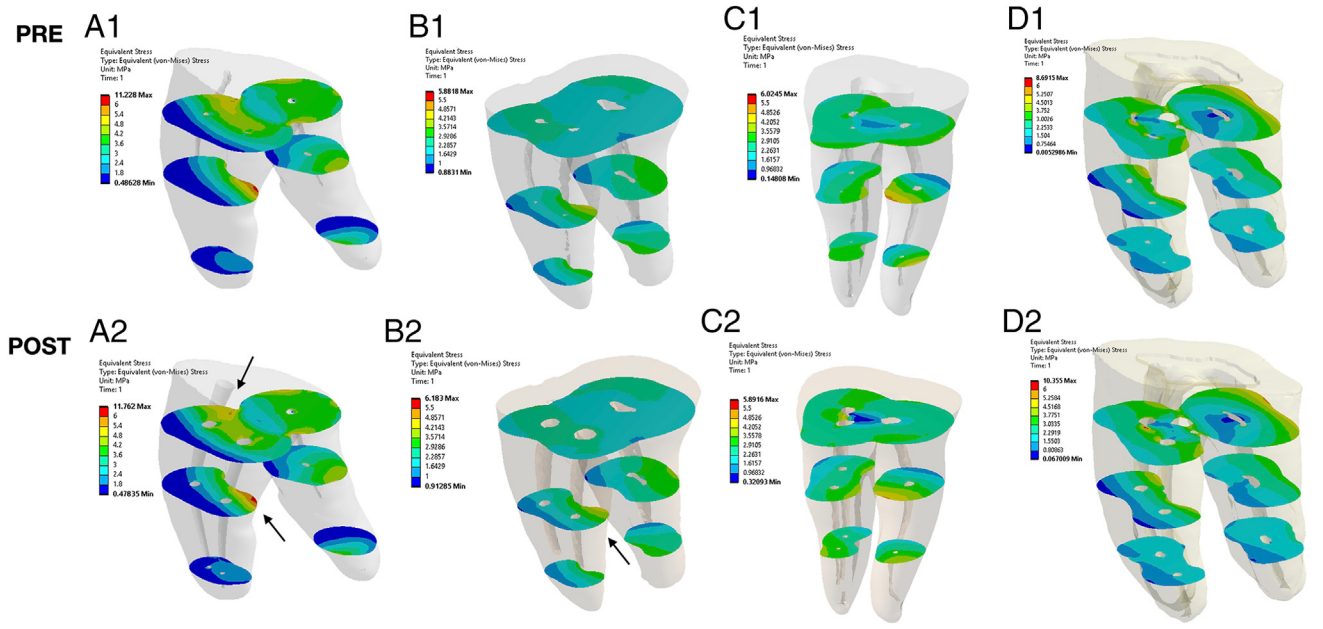

FIGURE 1 – The analysis of the pre- and postoperative equivalent von Mises stress distribution in the coronal, middle, and apical third for the different groups. *Blue* color indicates minimum stress and *red* indicates maximum stress (MPa scale). In the PG group, a slight increase of the von Mises stresses has been noticed at the point of analysis C and M ($P > .05$). Similarly, the PTN group showed an increase in the stress distribution at the point of analysis M ($P > .05$) (*arrows*). A1-A2: ProTaper Gold (taper 0.09). B1-B2: ProTaper Next (taper 0.06). C1-C2: B4U (taper 0.05). D1-D2: ProTaper Ultimate (taper 0.08).

The limits of this study include that despite the dentin being anisotropic, all simulated structures were considered to be isotropic and homogeneous. Therefore, only a qualitative analysis of the data was performed. Furthermore, the proposed FEM models produced results only for a possible anatomical situation, whereas the morphology and curvature of the roots, the height of the root, and other anatomical factors have influenced the location and distribution of stress. Finally, the presence of occlusal contacts and different

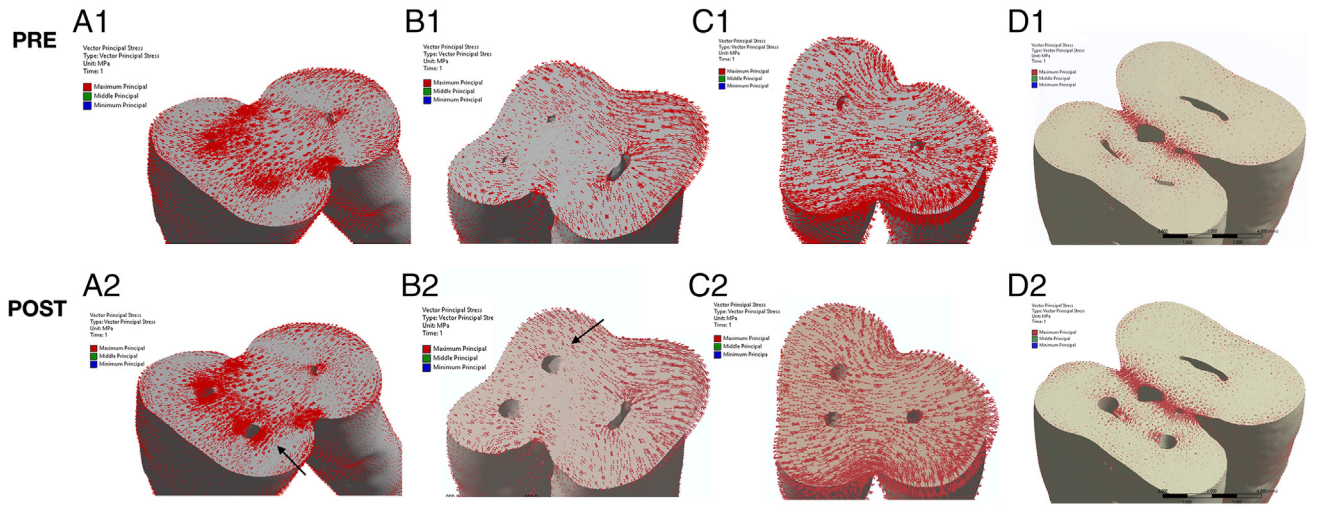

FIGURE 2 – The analysis of the pre- and postoperative vector distribution of the shear forces in the point of analysis D for the different groups. Vectors of the maximum principal stress are represented in red (MPa scale). In correspondence of the mesio-buccal canal of the PG model ($P = .021$) and the mesio-lingual canal of the PTN model ($P = .04$), the tension distribution showed significant increase (*arrows*). A1-A2: ProTaper Gold (taper 0.09). B1-B2: ProTaper Next (taper 0.06). C1-C2: B4U (taper 0.05). D1-D2: ProTaper Ultimate (taper 0.08).

physical-chemical dentinal properties could influence tooth fracture resistance.

CONCLUSION

The reduction of the root canal taper may improve the instruments' centering ability and the preservation of the residual dentin tissue, especially in the coronal and middle third. The root canal taper seems not to influence the stress distribution pattern through the mesial root of the lower molars.

ACKNOWLEDGMENTS

The micro-CT scans and FEM analysis were performed in collaboration with Dr Manuela Saba, Dr Vanessa Cucchiara, and Dr Filippo Dho. Prof. Damiano Pasqualini has been clinical advisor for Dentsply Sirona and Sweden & Martina in the past 5 years. The other authors deny any financial affiliation (eg, employment, direct payment, stock holdings, retainers, consultantships, patent licensing arrangements or honoraria), or involvement with any commercial organization with direct financial interest in the subject or materials discussed in this manuscript.

REFERENCES

1. Peters OA. Current challenges and concepts in the preparation of root canal systems: a review. J Endod 2004;30:559–67.
2. Hulsmann M, Peters OA, Dummer P. Mechanical preparation of root canals: shaping goals, techniques and means. Endod Top 2005;10:30–76.
3. Shen Y, Zhou HM, Zheng YF, et al. Current challenges and concepts of the thermomechanical treatment of nickel-titanium instruments. J Endod 2013;39:163–72.
4. Wang Q, Liu Y, Wang Z, et al. Effect of access cavities and canal enlargement on biomechanics of endodontically treated teeth: a finite element analysis. J Endod 2020;46:1501–7.
5. Silva E, Lima C, Barbosa A, et al. Influence of access cavity preparation on the dentine thickness of mesial canals of mandibular molars prepared with reciprocating instruments. Int Endod J 2022;55:113–23.
6. Barbosa A, Silva E, Coelho B, et al. The influence of endodontic access cavity design on the efficacy of canal instrumentation, microbial reduction, root canal filling and fracture resistance in mandibular molars. Int Endod J 2020;53:1666–79.
7. Elnaghy AM, Elsaka SE. Assessment of the mechanical properties of ProTaper Next Nickel-titanium rotary files. J Endod 2014;40:1830–4.
8. Zhao D, Shen Y, Peng B, Haapasalo M. Root canal preparation of mandibular molars with 3 nickel-titanium rotary instruments: a micro-computed tomographic study. J Endod 2014;40:1860–4.
9. Alovisi M, Cemenasco A, Mancini L, et al. Micro-CT evaluation of several glide path techniques and ProTaper Next shaping outcomes in maxillary first molar curved canals. Int Endod J 2017;50:387–97.
10. Arvaniti IS, Khabbaz MG. Influence of root canal taper on its cleanliness: a scanning electron microscopic study. J Endod 2011;37:871–4.
11. Aydin C, Tunca YM, Senses Z, et al. Bacterial reduction by extensive versus conservative root canal instrumentation *in vitro*. Acta Odontol Scand 2007;65:167–70.
12. Berutti E, Fedon G. Thickness of cementum/dentin in mesial roots of mandibular first molars. J Endod 1992;18:545–8.
13. Harris SP, Bowles WR, Fok A, McClanahan SB. An anatomic investigation of the mandibular first molar using micro-computed tomography. J Endod 2013;39:1374–8.
14. De-Deus G, Rodrigues EA, Belladonna FG, et al. Anatomical danger zone reconsidered: a micro-CT study on dentine thickness in mandibular molars. Int Endod J 2019;52:1501–7.
15. Pauletto G, Soares PM, Baumhardt T, et al. Effect of radiotherapy and taper of root canal preparation on the biomechanical behavior of mesial roots of mandibular molars. J Endod 2024;24:124–9.
16. Tantiwanichpun B, Kulvitit S. Efficiency and complications in root canal retreatment using nickel titanium rotary file with continuous rotation, reciprocating, or adaptive motion in curved root canals: a laboratory investigation. BMC Oral Health 2023;23:871.
17. Nagendrababu V, Murray PE, Ordinola-Zapata R, et al. PRILE 2021 guidelines for reporting laboratory studies in endodontology: a consensus-based development. Int Endod J 2021;54:1482–90.

18. Schneider SW. A comparison of canal preparations in straight and curved root canals. Oral Surg Oral Med Oral Pathol 1971;32:271–5.

19. Gu Y, Lu Q, Wang P, Ni L. Root canal morphology of permanent three-rooted mandibular first molars: Part II–measurement of root canal curvatures. J Endod 2010;36:1341–6.

20. Alovisi M, Pasqualini D, Musso E, et al. Influence of contracted endodontic access on root canal geometry: an *in vitro* study. J Endod 2018;44:614–20.

21. Cruz A, Vera J, Gascón G, et al. Debris remaining in the apical third of root canals after chemomechanical preparation by using sodium hypochlorite and glyde: an *in vivo* study. J Endod 2014;40:1419–23.

22. Jafarzadeh H, Abbott PV. Ledge formation: review of a great challenge in endodontics. J Endod 2007;33:1155–62.

23. Neves AA, Silva EJ, Roter JM, et al. Exploiting the potential of free software to evaluate root canal biomechanical preparation outcomes through micro-CT images. Int Endod J 2015;48:1033–42.

24. Baldi A, Scattina A, Ferrero G, et al. Highly-filled flowable composite in deep margin elevation: FEA study obtained from a microCT real model. Dent Mater J 2022;38:e94–107.

25. Kim S, Chen D, Park SY, et al. Stress analyses of retrograde cavity preparation designs for surgical endodontics in the mesial root of the mandibular molar: a finite element analysis-part II. J Endod 2020;46:539–44.

26. Rubin C, Krishnamurthy N, Capilouto E, et al. Stress analysis of the human tooth using a three-dimensional finite element model. J Dent Res 1983;62:82–6.

27. Smoljan M, Hussein MO, Guentsch A, Ibrahim M. Influence of progressive versus minimal canal preparations on the fracture resistance of mandibular molars: a 3-dimensional finite element analysis. J Endod 2021;47:932–8.

28. Tang W, Wu Y, Smales RJ. Identifying and reducing risks for potential fractures in endodontically treated teeth. J Endod 2010;36:609–17.

29. Reeh E, Messer H, Douglas W. Reduction in tooth stiffness as a result of endodontic and restorative procedures. J Endod 1989;15:512–6.

30. Gutmann JL. Minimally invasive dentistry (endodontics). J Conserv Dent 2013;16:282–3.

31. Ordinola-Zapata R, Martins JNR, Versiani MA, Bramante CM. Micro-CT analysis of danger zone thickness in the mesiobuccal roots of maxillary first molars. Int Endod J 2019;52:524–9.

32. Moore J, Fitz-Walter P, Parashos P. A micro-computed tomographic evaluation of apical root canal preparation using three instrumentation techniques. Int Endod J 2009;42:1057–64.

33. Belladonna FG, Guimarães TM, Silva EJ, et al. Exploring the efficacy of 6 preparation systems for achieving minimal root canal transportation: a micro-CT investigation. J Endod 2023;49:1722–32.

34. Pasqualini D, Bianchi CC, Paolino DS, et al. Computed micro-tomographic evaluation of glide path with nickel-titanium rotary PathFile in maxillary first molars curved canals. J Endod 2012;38:389–93.

35. Askerbeyli Örs S, Aksel H, Küçükkaya Eren S, Serper A. Effect of perforation size and furcal lesion on stress distribution in mandibular molars: a finite element analysis. Int Endod J 2019;52:377–84.

36. Zelic K, Vukicevic A, Jovicic G, et al. Mechanical weakening of devitalized teeth: three-dimensional finite element analysis and prediction of tooth fracture. Int Endod J 2015;48:850–63.

37. Sathorn C, Palamara JE, Palamara D, Messer HH. Effect of root canal size and external root surface morphology on fracture susceptibility and pattern: a finite element analysis. J Endod 2005;31:288–92.

38. Haapasalo M, Shen Y. Evolution of nickel-titanium instruments: from past to future. Endod Top 2013;29:3–17.

39. Keles A, Keskin C, Alqawasmi R, Versiani MA. Evaluation of dentine thickness of middle mesial canals of mandibular molars prepared with rotary instruments: a micro-CT study. Int Endod J 2020;53:519–28.